CS3: Large Strain Consolidation Model for Layered Soils

Patrick J. Fox, M.ASCE[1]; He-Fu Pu, S.M.ASCE[2]; and James D. Berles[3]

Abstract: A numerical model, called CS3, is presented for one-dimensional, large strain consolidation of layered soils. The algorithm accounts for vertical strain, soil self-weight, conventional constitutive relationships, changing material properties during consolidation, unload/reload, time-dependent loading and boundary conditions, an externally applied hydraulic gradient, and multiple soil layers with different material properties. CS3 can accommodate equilibrium and nonequilibrium profiles for the initial void ratio as well as variable profiles for preconsolidation stress and applied stress increment. Verification checks show excellent agreement with available analytical and numerical solutions. Several numeric examples are used to illustrate the capabilities of CS3 and highlight errors that may occur when multilayer systems are modeled as a single layer with average properties. Finally, settlement estimates obtained using CS3 are in good agreement with field measurements for the Gloucester test fill. **DOI: 10.1061/(ASCE)GT.1943-5606.0001128.**

Author keywords: Consolidation; Large strain; Layered soils; Numerical modeling; Clay.

Introduction

Fox and Berles (1997) presented a piecewise-linear numerical model called CS2 for one-dimensional, large strain consolidation of a single, homogeneous, saturated soil layer. CS2 accounts for vertical strain, general constitutive relationships, soil self-weight, relative velocity of fluid and solid phases, and changing material properties during consolidation. An enhanced version of CS2 with the ability to accommodate time-dependent loading, unload/reload, and an external hydraulic gradient was presented by Fox and Pu (2012). In the CS2 method, all variables pertaining to geometry, material properties, fluid flow, and effective stress are updated at each time step with respect to a fixed coordinate system. Mass conservation is strictly enforced using a Lagrangian approach that follows the motion of the solid phase throughout the consolidation process. Soil constitutive relationships are specified using discrete data points and do not require mathematical approximations or derivative functions. These features give CS2 high accuracy and considerable versatility to accommodate additional effects with excellent results. Using the CS2 method, subsequent large strain consolidation models have been developed to investigate accreting layers (Fox 2000), vertical and radial flows (Fox et al. 2003), compressible pore fluid (Fox and Qiu 2004), high-gravity conditions in a geotechnical centrifuge (Fox et al. 2005; Lee and Fox 2005), coupled solute transport (Fox 2007a, b; Fox and Lee 2008; Lee and Fox 2009), propagation of compression waves (Qiu and Fox 2008), and consolidation under a constant rate of strain (Pu et al. 2013; Fox et al. 2014). These studies have extensively verified the accuracy of the CS2 method using analytical solutions, numerical solutions, and experimental data, including solutions obtained using material coordinates (Gibson et al. 1967) and the moving boundary approach of Lee and Sills (1979). CS2 and related models have also been widely used by other researchers for new applications and to validate numerical analyses (Aydilek et al. 2000; Berilgen et al. 2000; Kokusho and Kojima 2002; Berilgen 2004; Bicer 2005; Berilgen et al. 2006; Kwon et al. 2007; Lewis 2009; Meric et al. 2010; Bharat and Sharma 2011; Lee and Park 2013). Most recently, the CS2 method has been adapted to model electro-osmotic consolidation (Zhou et al. 2013) and coupled contaminant transport (Meric et al. 2013) with impressive results.

An important capability not included in the preceding models is layered soil heterogeneity (i.e., multiple layers), which often occurs in practical applications. Previous research on consolidation of layered soils has been primarily conducted within the context of small (i.e., infinitesimal) strain theory. Assuming small strains, linear soil compressibility, and a constant coefficient of consolidation, Schiffman and Stein (1970) developed an analytical solution for one-dimensional consolidation of layered soils with general boundary conditions, initial conditions, and loading history. Lee et al. (1992) improved on this work and presented a more-explicit form of the solution. Other researchers have also made valuable contributions regarding consolidation modeling for layered soils under small strain conditions, including methods to account for depth-dependent loading (Zhu and Yin 1999a), partially drained boundaries (Xie et al. 1999), nonlinear soil compressibility (Xie et al. 2002), vertical and radial flows (Tang and Onitsuka 2001; Nogami and Li 2002, 2003; Wang and Jiao 2004; Walker et al. 2009), and various solution techniques, such as finite differences (Hazzard et al. 2008; Kim and Mission 2011), differential quadrature (Chen et al. 2005), matrix transfer (Nogami and Li 2002, 2003), and the spectral method (Walker et al. 2009). Perrone (1998) developed the elastoviscoplastic finite-element model CONSOL97, which can simulate consolidation of layered soils with time-dependent compressibility (i.e., creep) effects. This model uses an incremental, small strain approach with a coefficient of consolidation that varies with effective stress. Zhu and Yin (1999b) likewise developed a small strain, elastoviscoplastic model for layered clay soils using FEM. Mesri and Choi (1985) developed the finite-difference model ILLICON using finite-strain theory, which accounts for time-dependent loading, depth-dependent applied stress, changing material properties, and secondary compression.

[1]Professor, Dept. of Structural Engineering, Univ. of California–San Diego, La Jolla, CA 92093 (corresponding author). E-mail: pjfox@ucsd.edu

[2]Graduate Research Assistant, Dept. of Structural Engineering, Univ. of California–San Diego, La Jolla, CA 92093. E-mail: hepu@ucsd.edu

[3]Faculty Member, Alpena Community College, Alpena, MI 49707. E-mail: berlesj@alpenacc.edu

Note. This manuscript was submitted on September 1, 2012; approved on February 25, 2014; published online on April 28, 2014. Discussion period open until September 28, 2014; separate discussions must be submitted for individual papers. This paper is part of the ***Journal of Geotechnical and Geoenvironmental Engineering***, © ASCE, ISSN 1090-0241/04014041 (13)/$25.00.

Piecewise-linear consolidation models are generally considered to have excellent versatility with regard to initial conditions, boundary conditions, and material heterogeneity (Townsend and McVay 1990). This paper presents a piecewise-linear model for one-dimensional, large strain consolidation of layered soils called CS3 (Consolidation Settlement 3). CS3 has all the capabilities of the original CS2 (Fox and Berles 1997) and, in addition, accounts for layered heterogeneity, unload/reload effects, time-dependent loading and boundary head conditions, an external hydraulic gradient, and variable profiles for preconsolidation stress and applied stress increment. Constitutive relationships are defined in terms of conventional parameters, as opposed to individual data points in CS2, and allow for the direct input of laboratory and field data to facilitate modeling for practical applications. The development of CS3 is first described and then followed by verification checks. Several numeric examples are provided to show the effects of large strain, multiple layers, preconsolidation stress profile, and stress increment profile on soil consolidation behavior. Finally, settlement estimates obtained using CS3 are compared with field measurements for the Gloucester test fill.

Model Description

CS3 was developed using CS2 as a point of departure and follows similar procedures with regard to geometry, effective stress, fluid flow, and settlement (Berles 1995; Fox and Berles 1997; Fox and Pu 2012). The Lagrangian framework of CS2 is well suited for multilayer analysis because layer interfaces are automatically tracked and mass balance is satisfied by consideration of interlayer fluid flows. The following sections summarize the CS3 model with focus on its new capabilities.

Geometry

A saturated compressible soil stratum has initial height H_{To} and contains R_i horizontal layers. The initial geometry, prior to the application of load at time $t = 0$, is shown in Fig. 1. The stratum is sufficiently wide for all quantities to vary only in the vertical direction, and consolidation can be treated as one-dimensional. Vertical coordinate z and layer coordinate i are defined as positive upward from a fixed datum at the base of the stratum. Each layer i has initial height $H_{o,i}$, material properties given by a soil "sample" at initial elevation $z_{os,i}$, and $R_{j,i}$ vertical elements. The total number of elements for the stratum is $R_T = \sum_{i=1}^{R_i} R_{j,i}$. Layer elevation coordinate z_i and layer element coordinate j are defined as positive upward from the base of each layer. Each element j of layer i has unit cross-sectional area (plan view), initial height $L_{o,i}$, specific gravity of solids $G_{s,i}$, a central node at initial elevation $z_{o,i,j}$, and initial void ratio $e_{o,i,j}$. Nodes translate vertically and remain at the center of their respective elements throughout the consolidation process. Top and bottom boundaries for the stratum can be specified as drained or undrained, and if drained, are assigned initial total head values, h_{to} and h_{bo}, respectively, taken with respect to the datum. The stratum contains no internal drainage layers. Internal drainage layers can be treated by separately modeling each section of the stratum.

Constitutive Relationships

Rather than defining constitutive relationships using discrete data points as in CS2, which can be burdensome for multiple soil layers, constitutive relationships are defined in CS3 using conventional log-linear parameters for each layer. The compressibility relationship is shown in Fig. 2(a). Each element is characterized as normally consolidated (NC) or overconsolidated (OC). If NC, the compressibility relationship is defined by $e_{o,i,j}$ and compression index $C_{c,i}$. If OC, the compressibility relationship is defined by $e_{o,i,j}$, preconsolidation stress $\sigma'_{p,i,j}$, recompression index $C_{r,i}$, and $C_{c,i}$. The preconsolidation stress for an element is defined as the maximum past vertical effective stress at the corresponding node. Throughout a CS3 simulation, values of preconsolidation stress $\sigma'^{t}_{p,i,j}$ and corresponding void ratio $e^{t}_{p,i,j}$ are maintained for each element. If the vertical effective stress decreases below $\sigma'^{t}_{p,i,j}$, unloading and reloading follow an identical path defined by $\sigma'^{t}_{p,i,j}$, $e^{t}_{p,i,j}$, and $C_{r,i}$.

Hydraulic conductivity for each element is defined by a log-linear relationship between vertical hydraulic conductivity k and void ratio e, shown in Fig. 2(b), where $C'_{k,i} = \Delta \log k / \Delta e$ is the reciprocal of parameter C_k defined by Tavenas et al. (1983). CS3 uses the same hydraulic conductivity relationship for NC and OC conditions, which is consistent with the findings of Al-Tabbaa and Wood (1987), Nagaraj et al. (1994), and Fox (2007b). Aside from unload/reload effects, a one-to-one correspondence is assumed for each constitutive relationship in Fig. 2. Thus, CS3 does not account for the effects of strain rate, secondary compression, or aging on the compressibility or hydraulic conductivity of the soil.

Soil Sample Points

Material properties for each soil layer are defined at a single elevation, or "sample" point, within the layer (Fig. 1). Sample points may correspond to actual in situ soil sampling locations or fictitious locations chosen by the user based on other considerations. The following properties are constant for the ith soil layer and are taken from the corresponding ith soil sample: $G_{s,i}$, $C_{r,i}$, $C_{c,i}$, and $C'_{k,i}$. The following properties are also taken at the location of the ith soil sample but vary vertically within the layer: initial void ratio $e_{os,i}$, initial preconsolidation stress $\sigma'_{ps,i}$, and initial vertical hydraulic conductivity $k_{os,i}$. Soil sample properties can be measured using laboratory and field tests or estimated from empirical correlations (Azzouz et al. 1976; Kulhawy and Mayne 1990).

Preconsolidation Stress Profile

The profile of the preconsolidation stress σ'_p for each layer is characterized using one of four methods: (1) constant preconsolidation stress σ'_p, (2) constant overconsolidation ratio $(\mathrm{OCR}) = \sigma'_p/\sigma'_o$, (3) constant preconsolidation stress difference $\Delta\sigma' = \sigma'_p - \sigma'_o$, or (4) user-defined preconsolidation stress, where σ'_o is the initial vertical effective stress. Each method is illustrated in Fig. 3.

Initial Applied Stress Distribution

CS3 calculates the initial vertical total stress σ_o as the sum of soil self-weight and applied stresses at the top of the stratum. The initial applied effective stress at each node i, j consists of a depth-independent component q_o and a depth-dependent component $F_{i,j}p_o$, where p_o is the value at the top of the stratum, and $F_{i,j}$ is a fraction between 0 and 1 used to account for stress distribution effects with depth. Although not strictly applicable to 1D conditions, depth-dependent applied stress components are useful approximations for many practical applications. Values of $F_{i,j}$ are specified for the entire stratum using one of three methods: (1) linear, (2) bilinear, or (3) user-defined. Each method is illustrated in Fig. 4, where F_t, F_m, and F_b indicate values at the top, middle, and bottom of the stratum, respectively.

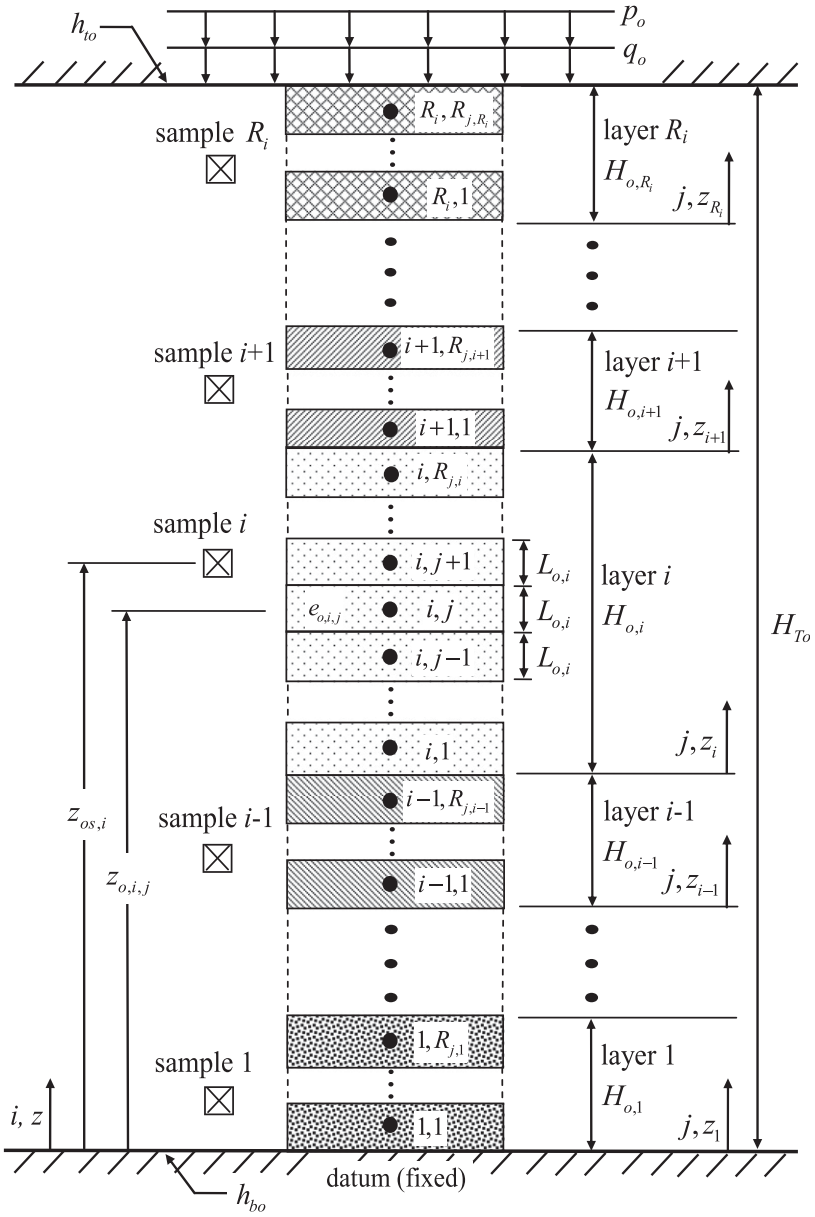

Fig. 1. Initial geometry for CS3

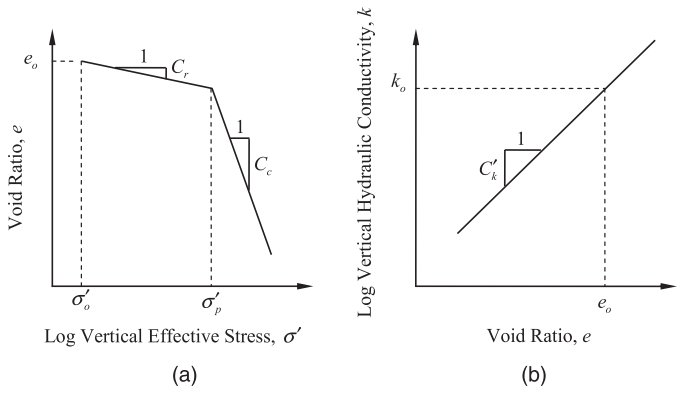

Fig. 2. Soil constitutive relationships: (a) compressibility; (b) hydraulic conductivity

Initial Void Ratio Distribution

A distribution of the initial void ratio is needed to begin a CS3 simulation. This distribution can be in equilibrium or non-equilibrium with initial stress conditions and soil material properties. Once obtained, the initial void ratio distribution is used to calculate a value of initial hydraulic conductivity for each element.

Equilibrium

Iteration is used to calculate an initial void ratio distribution within each layer that is in equilibrium with initial stress conditions, soil self-weight and constitutive relationships, and seepage forces due to an external hydraulic gradient acting across the stratum (if $h_{to} \neq h_{bo}$). In this case, initial excess pore pressures (i.e., the differences between the total and steady-state pore pressures) are zero. For the first iteration loop, CS3 calculates the initial buoyant unit weight of each ith soil sample as $\gamma'_{os,i} = \gamma_w(G_{s,i} - 1)/(1 + e_{os,i})$. Using these values and starting at the top of the stratum with known values of q_o, p_o and

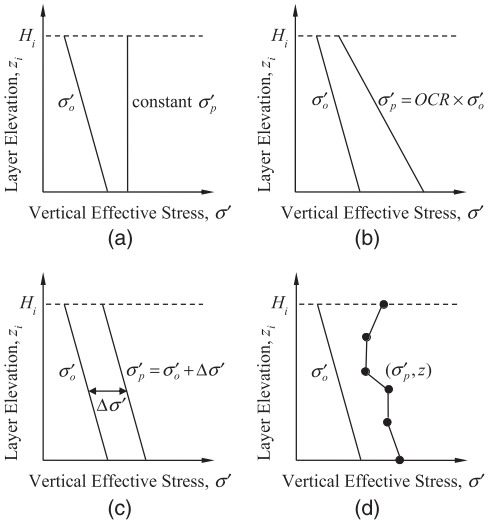

Fig. 3. Profiles for preconsolidation stress: (a) constant σ'_p; (b) constant OCR; (c) constant $\Delta\sigma'$; (d) user-defined

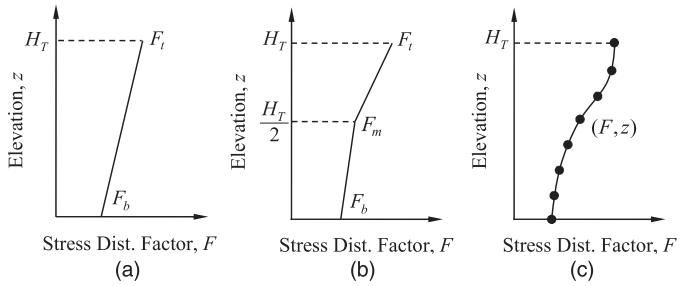

Fig. 4. Profiles for stress distribution factor: (a) linear; (b) bilinear; (c) user-defined

$F_{i,j}$, the initial vertical effective stress is calculated at each sample location $\sigma'_{os,i}$ and at the node for each element $\sigma'_{o,i,j}$. CS3 uses the initial condition of sample i ($\sigma'_{os,i}$, $e_{os,i}$), along with $C_{r,i}$, $C_{c,i}$, $\sigma'_{p,i,j}$, and $\sigma'_{o,i,j}$, to estimate the initial void ratio $e_{o,i,j}$ for all elements in each layer i. These estimates are then used to recalculate the initial buoyant unit weight of each element $\gamma'_{o,i,j}$, which yields new values of $\sigma'_{os,i}$, $\sigma'_{o,i,j}$, and $e_{o,i,j}$. This process is repeated until changes in $\sigma'_{o,s,i}$ and $\sigma'_{o,i,j}$ become negligible for successive iterations. If an external hydraulic gradient is present, the iteration procedure includes an additional loop to account for associated seepage forces (Fox and Pu 2012).

Nonequilibrium

CS3 can also accommodate a user-defined distribution of initial void ratio. The most common example is a uniform e_o profile. User-defined initial void ratios will generally not be in equilibrium with initial conditions and soil material properties, which produces non-zero values of excess pore pressure within the stratum at the start of loading.

Application of Surcharge Load

Surcharge load is applied to the stratum beginning at $t = 0$. The vertical effective stress at the top boundary is equal to $q^t + p^t$, where $q^t = q_o + \Delta q^t$, and $p^t = p_o + \Delta p^t$, and effective stress increments Δq^t and Δp^t can vary independently with time. The value of Δq^t is constant with depth, whereas the value of Δp^t changes with depth according to stress distribution factor $F_{i,j}$ (Fig. 4). Thus, the applied effective stress at node i,j is equal to $q^t + F_{i,j}p^t$, where values of $F_{i,j}$ are assumed to remain constant during consolidation. Boundary head values, h_t^t and h_b^t, can also vary independently with time. In response to surcharge loading, excess pore pressures generated within the layer cause fluid flow to all drainage boundaries. Soil deformation is one-dimensional and occurs in response to the net fluid outflow from each element. Void ratio is assumed to remain uniform within each element throughout the consolidation process. At time t, the total height of the stratum is H_T^t, the height of the ith layer is H_i^t, the height of the jth element is $L_{i,j}^t$, and the elevation of any node i,j is $z_{i,j}^t$.

Stress, Pore Pressure, Fluid Flow, and Settlement

The vertical total stress at node i,j is obtained from the applied stress conditions and self-weight of overlying elements

$$\sigma_{i,j}^t = q^t + F_{i,j}p^t + \left(h_t^t - H_T^t\right)\gamma_w + \frac{L_{i,j}^t\gamma_{i,j}^t}{2} + \sum_{b=j+1}^{R_{j,i}} L_{i,b}^t\gamma_{i,b}^t + \sum_{a=i+1}^{R_i}\sum_{b=1}^{R_{j,a}} L_{a,b}^t\gamma_{a,b}^t, \quad i = 1,2,\ldots,R_i;\ j = 1,2,\ldots,R_{j,i} \tag{1}$$

where $\gamma_{i,j}^t = \gamma_w[(G_{s,i} + e_{i,j}^t)/(1 + e_{i,j}^t)]$ = saturated unit weight of element i,j; and $e_{i,j}^t$ = corresponding void ratio. Vertical effective stress $\sigma'^t_{i,j}$ is calculated from $e_{i,j}^t$ and the compressibility relationship of the corresponding layer. Unload/reload effects are taken into account if $\sigma'^t_{i,j} < \sigma'^t_{p,i,j}$.

The pore pressure at node i,j is the difference between total and effective stresses

$$u_{i,j}^t = \sigma_{i,j}^t - \sigma'^t_{i,j}, \quad i = 1,2,\ldots,R_i;\ j = 1,2,\ldots,R_{j,i} \tag{2}$$

Pore pressures are used to calculate fluid flow between contiguous elements. The relative discharge velocity (positive upward) between nodes i,j and $i,j+1$ is

$$v_{rf,i,j}^t = -\left[\frac{k_{i,j+1}^t k_{i,j}^t\left(L_{i,j+1}^t + L_{i,j}^t\right)}{L_{i,j+1}^t k_{i,j}^t + L_{i,j}^t k_{i,j+1}^t}\right]\left(\frac{h_{i,j+1}^t - h_{i,j}^t}{z_{i,j+1}^t - z_{i,j}^t}\right), \quad i = 1,2,\ldots,R_i;\ j = 1,2,\ldots,R_{j,i} - 1 \tag{3}$$

where $h_{i,j}^t = z_{i,j}^t + (u_{i,j}^t/\gamma_w)$ = total hydraulic head at node i,j; and $k_{i,j}^t$ = vertical hydraulic conductivity of element i,j. Corresponding expressions are used at interfaces between contiguous layers (i.e., between node $i,R_{j,i}$ and node $i+1,1$), as well as at the top and bottom boundaries of the stratum.

Once the relative discharge velocities are known, a new height is calculated for each element from the net fluid outflow over time increment Δt

$$L_{i,j}^{t+\Delta t} = L_{i,j}^t - \left(v_{rf,i,j}^t - v_{rf,i,j-1}^t\right)\Delta t, \quad i = 1,2,\ldots,R_i;\ j = 1,2,\ldots,R_{j,i} \tag{4}$$

where Δt is defined by Fox and Pu (2012). New values of void ratio, layer height, stratum height, settlement, and average degree of consolidation are then calculated as

$$e_{i,j}^{t+\Delta t} = \frac{L_{i,j}^{t+\Delta t}\left(1 + e_{o,i,j}\right)}{L_{o,i}} - 1, \quad i = 1, 2, \ldots, R_i;\ j = 1, 2, \ldots, R_{j,i} \tag{5}$$

$$H_i^{t+\Delta t} = \sum_{j=1}^{R_{j,i}} L_{i,j}^{t+\Delta t}, \quad i = 1, 2, \ldots, R_i \tag{6}$$

$$H_T^{t+\Delta t} = \sum_{i=1}^{R_i} H_i^{t+\Delta t} \tag{7}$$

$$S^{t+\Delta t} = H_{To} - H_T^{t+\Delta t} \tag{8}$$

$$U_{\text{avg}}^{t+\Delta t} = \frac{S^{t+\Delta t}}{S_{\text{ult}}} \tag{9}$$

where S_{ult} = ultimate settlement corresponding to 100% consolidation. The final void ratio distribution, and hence S_{ult}, can be calculated at the beginning of a simulation if the final data point is the largest value in the surcharge loading schedule. Otherwise, unloading will occur, S_{ult} will not be known a priori, and U_{avg} values are not calculated during the course of a simulation.

The preceding method ensures that the weight of solids contained within each element is invariant throughout the consolidation process (Fox and Berles 1997). Solid particles do not cross from one element to the next, and element nodes and interfaces, as well as layer interfaces, can be considered as embedded in the soil skeleton. As such, the method follows the motion of the solid phase and consideration of relative discharge velocity between contiguous elements is sufficient to ensure mass balance.

Model Performance

Verification

Example 1 is used to compare the results of CS3 simulations with those obtained using small strain theory. A double-drained clay stratum has an initial total height of 11 m, contains three layers, and is in equilibrium under an initial effective overburden stress of 40 kPa. Layer properties are provided in Table 1, where $a_{v,i}$ is the coefficient of compressibility $(-\Delta e/\Delta\sigma')$ for layer i, and soil sample locations are taken at the midheight of each layer. Total heads at the top and bottom boundaries are 11 m (constant), soil self-weight is neglected ($G_s = 1$), and the initial void ratio is constant within each layer. At $t = 0$, a uniform ($p = 0$), instantaneous, and very small vertical effective stress increment of $\Delta q = 0.001$ kPa is applied to the stratum, which yields a final average strain of 2.6×10^{-6}. The coefficient of compressibility, hydraulic conductivity, and coefficient of consolidation $c_{v,i}$ are constant for each layer during consolidation. A small modification to CS3 was necessary to accommodate constant values of a_v. Table 2 compares values of U_{avg} obtained as a function of time from the analytical solution of Lee et al. (1992) and four CS3 simulations performed for $R_{j,i}$ = 50, 100, 200, and 300.

Table 1. Soil Layer Properties for Examples 1 and 2

Layer i	$H_{o,i}$ (m)	$z_{os,i}$ (m)	$e_{os,i}$	$a_{v,i}$ ($\times 10^{-3}$/kPa)	$k_{os,i}$ ($\times 10^{-9}$ m/s)	$C'_{k,i}$
1	4	2	0.8	3	2	0
2	5	6.5	1.5	9	20	0
3	2	10	1.2	4	4	0

Values are in good to excellent agreement and the accuracy of CS3 improves with increasing numerical resolution (i.e., increasing R_T). Table 3 compares vertical profiles of excess pore pressure for elapsed times of 36, 650, and 2,400 days, which approximately correspond to U_{avg} = 10, 50, and 90%, respectively. Values obtained from CS3 ($R_{j,i} = 100$; $R_T = 300$) are essentially in exact agreement with the analytical solutions.

No analytical solutions exist for large strain consolidation of layered soils. However, CS2 produces results that are essentially identical to analytical solutions for large strain consolidation of a single layer (Fox and Berles 1997), and CS3 simulations exactly match those obtained from CS2 for $R_i = 1$. This agreement, and the above agreement for small strains, which indicates that CS3 correctly handles boundary and layer interface conditions, strongly suggests that CS3 is valid for the simulation of large strain consolidation of layered soils.

Parametric Study

Large Strain

Example 2 shows the effect of large strain on the rate of consolidation for the same soil stratum as described in Table 1. Three simulations were conducted using CS3 ($R_{j,i} = 200$), and the results are shown in Fig. 5. Values of U_{avg} for the first simulation correspond to small strain conditions, with $\Delta q = 0.001$ kPa and constant soil properties, as in Table 1. For the second simulation, soil properties were unchanged, but the stress increment was increased to Δq = 100 kPa to yield a final settlement of 2.83 m and a final vertical strain of 26%. Fig. 5 indicates that the rate of settlement for this case increases slightly due to the progressively shorter drainage distance for pore water outflow from the stratum. The third simulation was identical to the second except that hydraulic conductivity was permitted to decrease with void ratio according to $C'_{k,i} = 2/e_{os,i}$, which reflects realistic conditions for many clay soils (Tavenas et al. 1983; Mesri et al. 1994). Allowing for variable hydraulic conductivity produces a fourfold increase in the time for $U_{\text{avg}} = 95\%$ as compared with the large strain case with constant k.

Multiple Layers

Example 3 shows the effect of multiple layers on consolidation behavior. A double-drained stratum is defined by $H_{To} = 9$ m, G_s = 2.7, $q_o = 20$ kPa, $h_t = h_b = 9$ m (constant), and the remaining values in Table 4. The distribution of initial void ratio is in equilibrium with applied stress conditions and soil self-weight. An instantaneous and constant stress increment of $\Delta q = 250$ kPa is applied to the stratum and is uniform with depth ($p = 0$). CS3 simulations were conducted for three cases ($R_T = 300$). Case 1 models the stratum as a single layer. Cases 2 and 3 model the stratum using three layers with initial heights of 3 m and varying material properties. Case 3 considers a larger range of initial void ratio and compressibility and hydraulic conductivity properties than Case 2; however, average parameter values for both Cases 2 and 3 are equal to those for Case 1. The preconsolidation stress is initially constant within each layer.

Fig. 6 presents settlement and settlement ratio versus time for Example 3, where the settlement ratio is defined as the settlement for Case 1 (single layer stratum) divided by the settlement for Case 2 or Case 3 (multilayer stratum). The use of compressibility properties with consistent average values produces final settlements that are nearly equal for all three cases. Prior to final settlement, maximum values of settlement ratio are 1.06 and 1.19 for Cases 2 and 3, respectively. Consolidation for Cases 2 and 3 occurs more slowly than for Case 1, which results from the preponderant effect of lower

Table 2. Average Degree of Consolidation for Example 1

Time, t (days)	Average degree of consolidation, U_{avg} (%)				
	Lee et al. (1992) theory	CS3: $R_{j,i} = 50$; $R_T = 150$	CS3: $R_{j,i} = 100$; $R_T = 300$	CS3: $R_{j,i} = 200$; $R_T = 600$	CS3: $R_{j,i} = 300$; $R_T = 900$
1	1.692	1.662	1.685	1.691	1.692
5	3.784	3.772	3.781	3.783	3.784
10	5.352	5.343	5.350	5.351	5.351
50	11.978	11.974	11.977	11.978	11.978
100	17.128	17.125	17.127	17.128	17.128
500	43.649	43.648	43.649	43.649	43.649
1,000	64.510	64.509	64.510	64.510	64.510
5,000	99.113	99.113	99.113	99.113	99.113

Table 3. Excess Pore Pressure Profiles for Example 1

Elevation z	Excess pore pressure, u_{ex} ($\times 10^{-4}$ kPa)					
	$t = 36$ days		$t = 650$ days		$t = 2{,}400$ days	
	Lee et al. (1992) theory	CS3	Lee et al. (1992) theory	CS3	Lee et al. (1992) theory	CS3
10.01	6.036	6.036	2.591	2.591	0.517	0.517
9.01	9.539	9.539	5.087	5.087	1.015	1.015
8.025	9.870	9.870	5.531	5.531	1.103	1.103
7.025	9.971	9.971	5.861	5.861	1.169	1.169
6.025	9.995	9.995	6.081	6.081	1.212	1.212
5.025	9.999	9.999	6.188	6.188	1.233	1.233
4.025	10.000	10.000	6.178	6.178	1.230	1.230
3.02	9.995	9.995	5.235	5.235	1.034	1.034
2.02	9.794	9.794	3.806	3.806	0.747	0.747
1.02	7.576	7.577	2.020	2.020	0.394	0.394

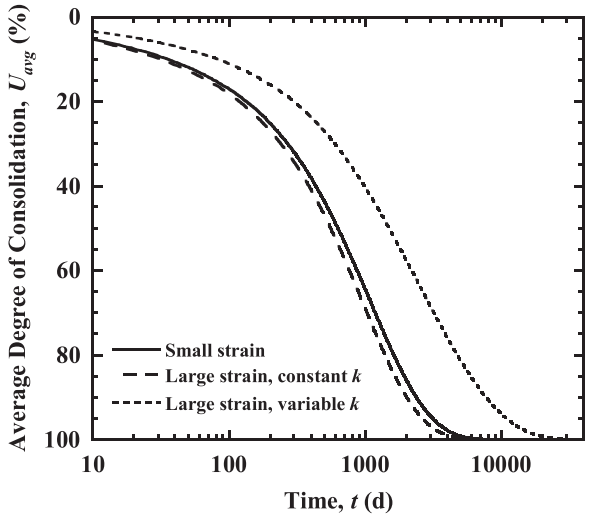

Fig. 5. Average degree of consolidation for Example 2

hydraulic conductivity in Layer 1 for the multilayer simulations. Fig. 7 compares profiles of excess pore pressure u_{ex} at 30, 300, and 1,000 days. At $t = 0$, the initial excess pore pressure is uniform and equal to the applied surcharge (250 kPa) for each case. Pressures then dissipate in response to the distribution of material properties within the stratum. At $t = 30$ days, the Case 1 profile displays slight asymmetry due to the effect of soil self-weight and the transition from OC conditions near the center to NC conditions near the

Table 4. Soil Layer Properties for Example 3

Case	Layer i	$H_{o,i}$ (m)	$z_{os,i}$ (m)	$e_{os,i}$	$\sigma'_{ps,i}$ (kPa)	$C_{c,i}$	$C_{r,i}$	$k_{os,i}$ ($\times 10^{-9}$ m/s)	$C'_{k,i}$
1	1	9	4.5	2.5	100	1	0.1	2	0.8
2	1	3	1.5	2	125	1.25	0.125	1	1
	2	3	4.5	2.5	100	1	0.1	2	0.8
	3	3	7.5	3	75	0.75	0.075	3	0.6
3	1	3	1.5	1.5	150	1.5	0.15	0.5	1.1
	2	3	4.5	2.5	100	1	0.1	2	0.8
	3	3	7.5	3.5	50	0.5	0.05	3.5	0.5

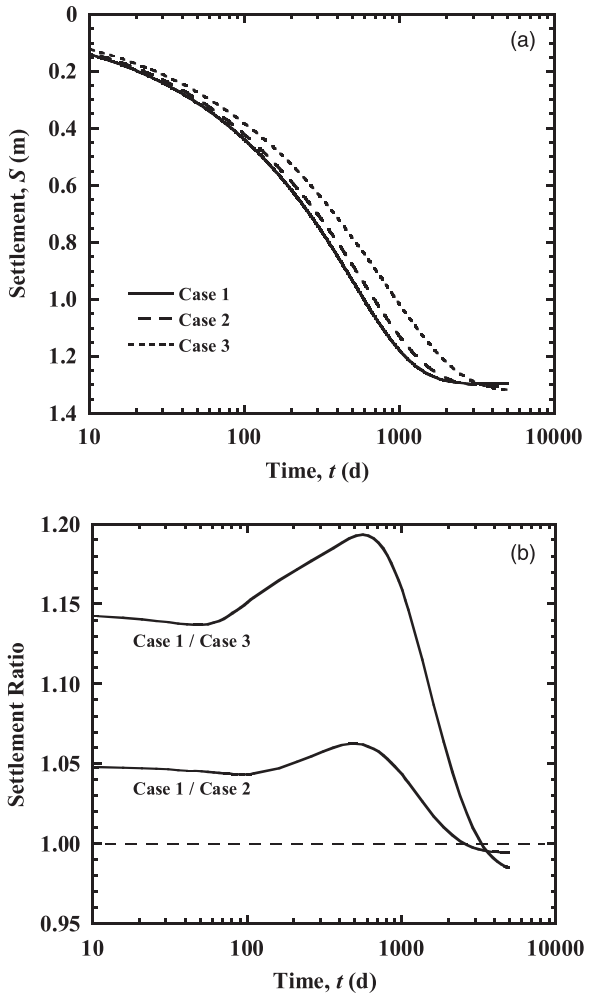

Fig. 6. Comparison of three cases for Example 3: (a) settlement; (b) settlement ratio

boundaries. Corresponding profiles for Cases 2 and 3 show greater asymmetry due to greater soil heterogeneity. With increasing time, the effect of low hydraulic conductivity for Layer 1 becomes more pronounced for the multilayer simulations and causes the location of maximum excess pore pressure to skew toward the bottom of the stratum.

Preconsolidation Stress Profile

Example 4 investigates the effect of preconsolidation stress profile. A single layer is defined by Case 1 in Example 3 and by the three preconsolidation stress profiles shown in Fig. 8. The profiles pass through a common point at the midheight of the layer and correspond to constant $\sigma'_p = 100$ kPa, constant OCR = 2.42, and constant $\Delta\sigma' = 58.6$ kPa. Settlement curves are shown in Fig. 9 and indicate that, with the same average σ'_p, settlements are nearly identical. However, other simulations (not shown) have indicated larger deviations when the common point occurs either above or below the midheight of the layer and the average σ'_p value is not the same. Profiles of excess pore pressure are shown in Fig. 10 for 30, 300, and 1,000 days. Surcharge loading again produces a uniform initial excess pore pressure of 250 kPa. Thereafter, the curves display trends consistent with the initial distribution of $\sigma'_p - \sigma'_o$. Higher excess pore pressures are observed at locations with lower initial values of $\sigma'_p - \sigma'_o$ because the soil transitions to NC earlier in the consolidation process. This transition produces a corresponding increase in compressibility and reduction in hydraulic conductivity, both of which slow the process of excess pore pressure dissipation.

Stress Increment Profile

To investigate the effect of stress reduction with depth, Example 5 again considers a single layer defined by Case 1 in Example 3. The layer is subjected to a finite-area loading. Using elastic theory, the loading yields the stress increment profile shown in Fig. 11 and includes vertical stress increments at the top $\Delta\sigma_t$, middle $\Delta\sigma_m$, and bottom $\Delta\sigma_b$ of 250, 118, and 55 kPa, respectively. Five other stress increment profiles are also shown: (1) uniform $\Delta q = 250$ kPa, (2) linear [Fig. 4(a)], (3) uniform approximation ($\Delta q_{avg} = 152.2$ kPa) to

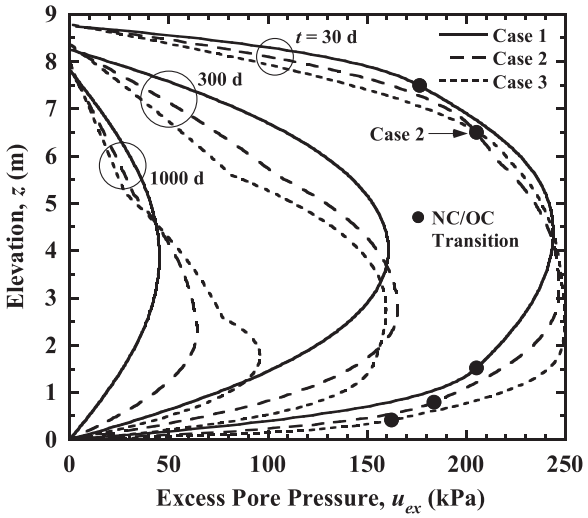

Fig. 7. Excess pore pressure profiles for Example 3

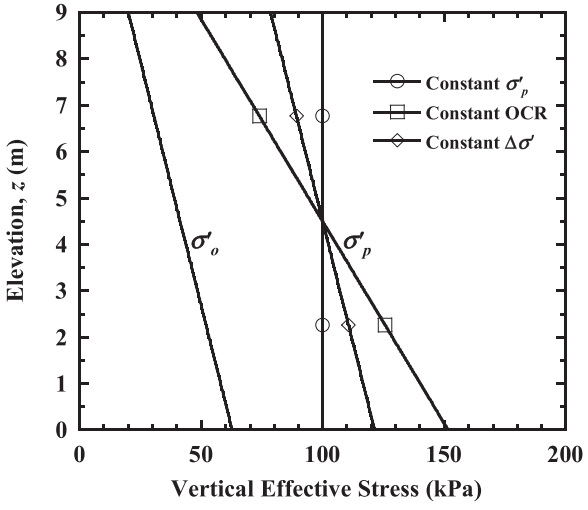

Fig. 8. Profiles of initial effective stress and preconsolidation stress for Example 4

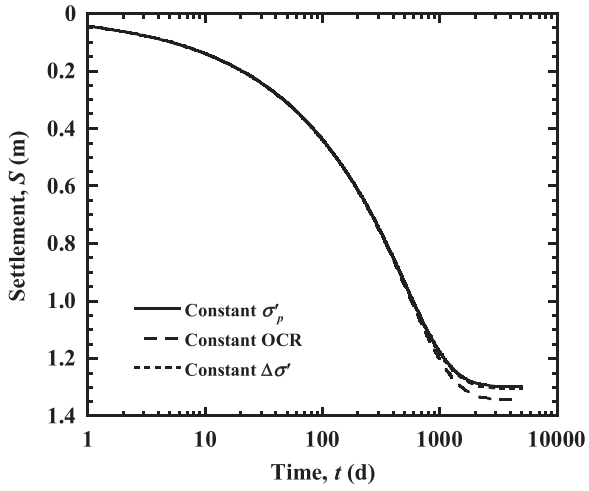

Fig. 9. Settlement curves for Example 4

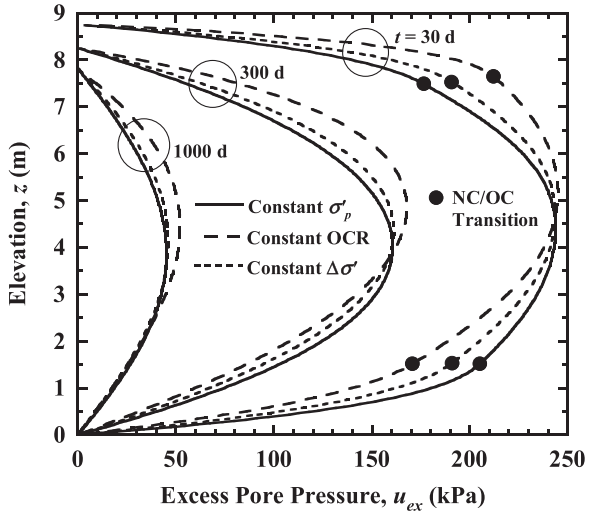

Fig. 10. Excess pore pressure profiles for Example 4

linear, (4) bilinear [Fig. 4(b)], and (5) uniform approximation ($\Delta q_{avg} = 129.5$ kPa) to bilinear. Uniform approximations to the linear and bilinear stress increment profiles were calculated as weighted averages using Simpson's rule

$$\Delta q_{avg} = \frac{\Delta\sigma_t + 4\Delta\sigma_m + \Delta\sigma_b}{6} \quad (10)$$

CS3 simulations for settlement are shown in Fig. 12. The elastic theory profile was modeled using 43 data points [Fig. 4(c)] and yields a final settlement of 0.68 m. The uniform $\Delta q = 250$ kPa profile yields a final settlement of 1.3 m and indicates that failure to consider applied stress reduction with depth can produce significant errors in calculated settlements. Settlements for the linear and bilinear profiles are also overestimated but are in closer agreement to settlements calculated using the elastic theory profile (final settlement error is 20% for linear and 4% for bilinear). Interestingly, uniform loading using the Simpson's rule approximation produces very close estimates of settlement for the linear and bilinear profiles in this example. Likewise, it is also interesting that U_{avg} curves (not shown) are essentially identical for all six stress increment profiles. However, corresponding excess pore pressures for $t = 30$ days, shown in Fig. 13, indicate that although the settlement curves may be in close agreement, excess pore pressures generated using Simpson's rule approximations, which do not capture the initial variation of excess pore pressure with depth, can be in substantial error.

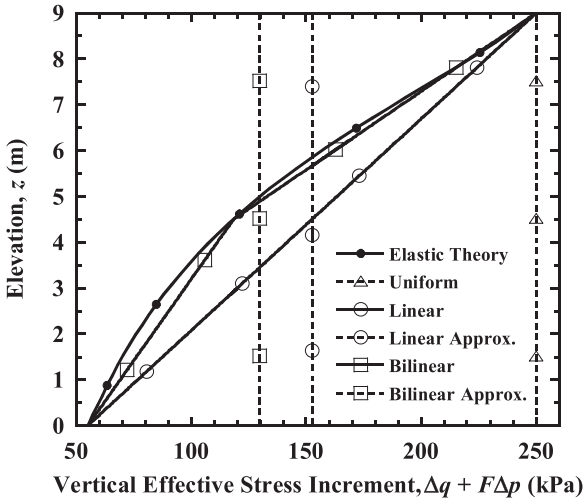

Fig. 11. Stress increment profiles for Example 5

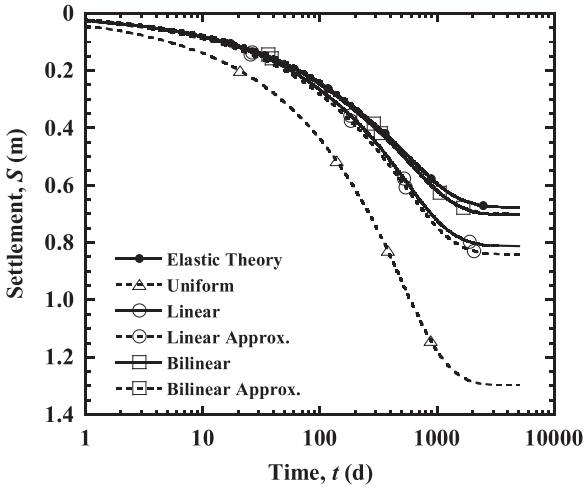

Fig. 12. Settlement curves for Example 5

Case Study

The Gloucester test fill was constructed in 1967 by the National Research Council of Canada at a location 21 km south of Ottawa, Canada. Information and data for the project were obtained primarily from Bozozuk (1972), Bozozuk and Leonards (1972), Lo et al. (1976), Leroueil et al. (1983), and Hinchberger and Rowe (1998). Subsurface conditions are described in Table 5. The upper 1.8 m consisted of top soil and a thin desiccated crust. Below the crust were six layers of marine silty clays with sensitivity values ranging from approximately 10 to 100. The sensitive clays were underlain by a firm drained boundary at a depth of 20.2 m (Hinchberger and Rowe 1998). Subsurface profiles of initial water content, Atterberg limits, initial void ratio, initial vertical hydraulic conductivity, compression index, recompression index, and preconsolidation pressure are shown in Figs. 14–18. The groundwater table was located near the ground surface and experienced seasonal fluctuations (Bozozuk 1972; Leroueil et al. 1983).

In August 1967, a shallow excavation was made on the site to a depth of 1.2 m, which removed the top soil layer and part of the desiccated crust and produced a stress release of 24.2 kPa. One month later, the Gloucester fill was constructed inside the excavation. The fill had a height of 3.7 m, a top width of 9.1 m, a base width of 20.1 m, and a length equal to approximately twice the width. The applied stress at the base of the fill under the centerline was 67.7 kPa (Bozozuk and Leonards 1972). Settlement gauges S1, S2, and S3 were installed under the centerline at depths of 0.30 m, 1.22 m, and 3.66 m, respectively, below the base of the fill. Total settlement measurements are presented in Fig. 19 and, after almost 5,000 days, indicate values of 0.33, 0.26, and 0.12 m at these depths.

The compressible stratum for the Gloucester test fill was considered as the lower seven layers in Table 5 (i.e., from depth 0.8 m to depth 20.2 m). Four simulations were conducted using CS3 to

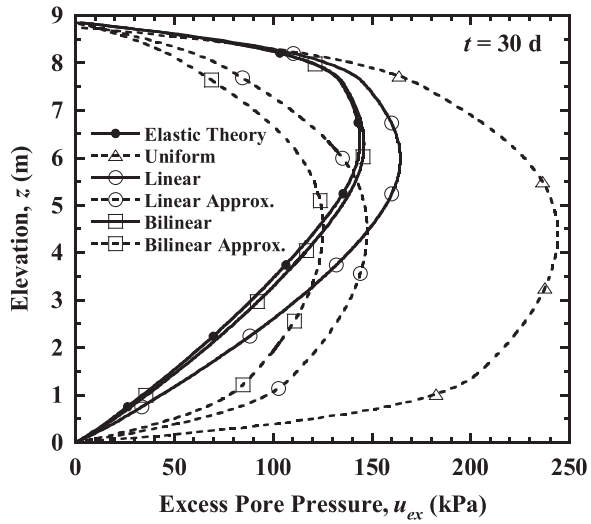

Fig. 13. Excess pore pressure profiles for Example 5

Table 5. Subsurface Conditions for Gloucester Test Fill

Soil profile[a]	Depth (m)	Layer i	$H_{o,i}$ (m)	$z_{os,i}$ (m)	Layer average values					
					$e_{o,i}$	$C_{c,i}$	$C_{r,i}$	$k_{o,i}$ ($\times 10^{-9}$ m/s)	$C'_{k,i}$[b]	A_i
Black organic top soil; tan fine sand and silt	0–0.8	—	—	—	—	—	—	—	—	—
Desiccated gray-brown silty clay	0.8–1.8	7	0.61	18.68	2.04	1.32	0.096	6.25	0.20	1.47
Soft gray-brown silty clay; occasional decayed roots and small flat stones	1.8–2.7	6	0.91	17.92	1.97	1.65	0.076	1.25	0.27	1.47
Soft gray silty clay; some shells	2.7–5.3	5	2.59	16.17	1.93	1.70	0.075	1.25	0.43	1.76
Gray silty clay; some shells	5.3–7.0	4	1.68	14.03	1.59	0.89	0.075	1.25	0.35	0.81
Gray clay with black mottling; occasional small flat stones	7.0–13.9	3	6.86	9.76	2.41	3.06	0.079	1.0	0.38	3.10
Gray silty clay with black mottling; occasional shells and small stones	13.9–18.3	2	4.42	4.12	1.66	1.54	0.055	1.25	0.26	4.58
Gray varved clay and silt; heterogeneous deposit of gray clay, silt, fine sand, and small stones	18.3–20.2	1	1.91	0.96	1.71	1.62	0.066	1.25	0.26	0.00

[a]Soil profile data from Bozozuk (1972).
[b]C'_k calculated from Table B-3 of Bozozuk (1972).

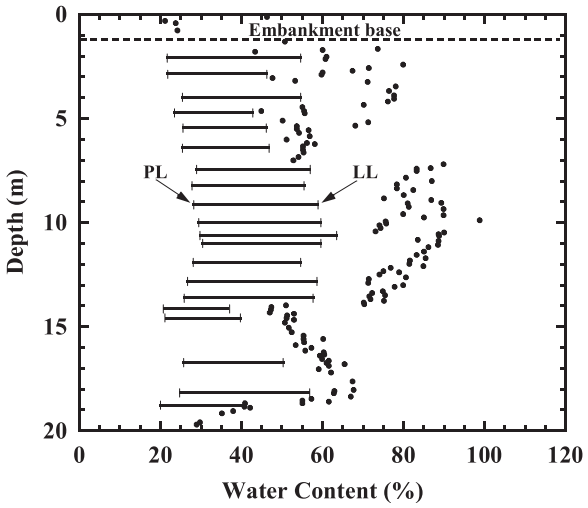

Fig. 14. Subsurface profiles of initial water content and Atterberg limits (data points scaled from Fig. 3 of Bozozuk 1972)

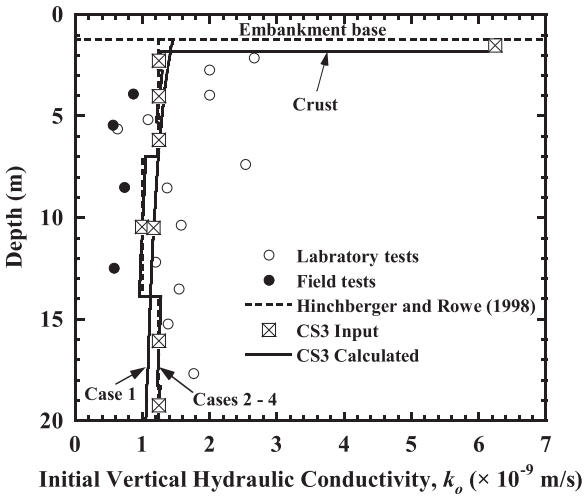

Fig. 16. Subsurface profile of initial vertical hydraulic conductivity (laboratory test data points from Table B-3 of Bozozuk 1972; field test data points scaled from Fig. 9 of Hinchberger and Rowe 1998)

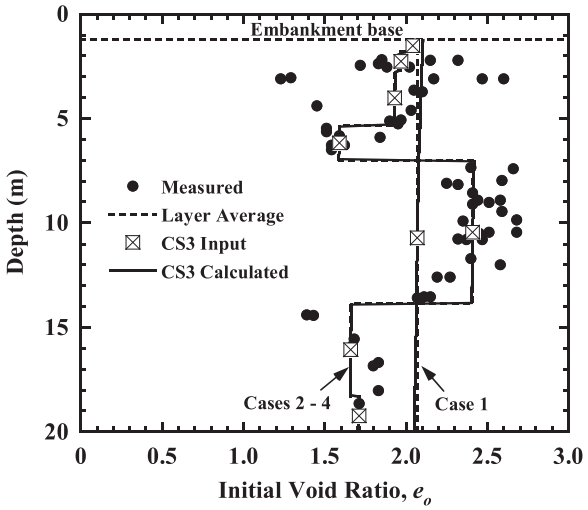

Fig. 15. Subsurface profile of initial void ratio (data points scaled from Fig. 23 of Bozozuk 1972)

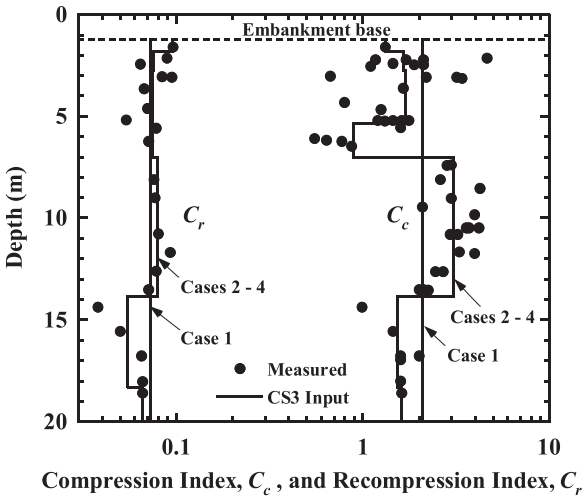

Fig. 17. Subsurface profiles of compression index and recompression index (C_c data points scaled from Fig. 23 of Bozozuk 1972; C_r data points calculated from Appendix B of Bozozuk 1972)

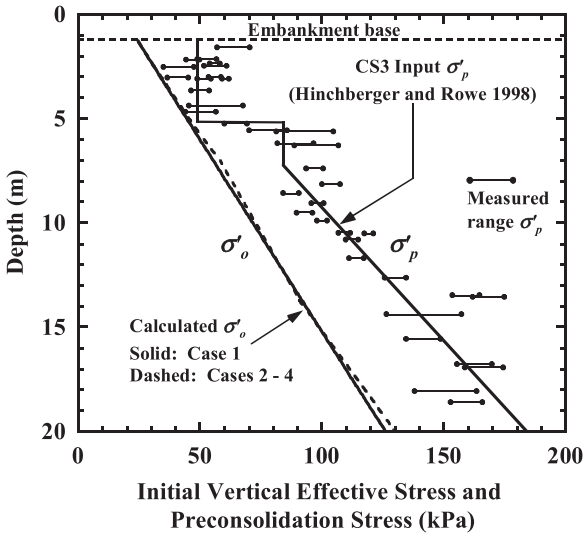

Fig. 18. Subsurface profiles of initial vertical effective stress and preconsolidation stress (data points scaled from Fig. 3 of Bozozuk 1972)

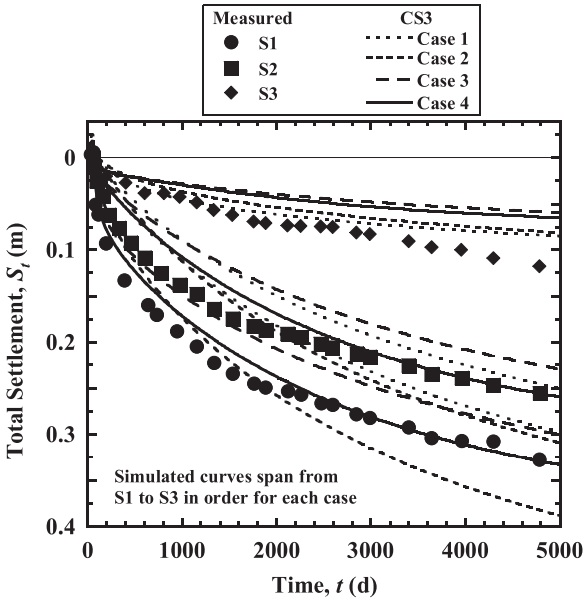

Fig. 19. Settlement curves for Gloucester test fill (data points for first 4 years scaled from Fig. D-1 of Bozozuk 1972; remaining data points scaled from Fig. 11 of Hinchberger and Rowe 1998)

calculate settlements (Table 6). Total heads at the top and bottom of the stratum were based on a groundwater table at a constant depth of 1.8 m (base of crust), the initial void ratio profile was assumed to be in equilibrium with initial conditions, and unloading/loading was applied in the correct time sequence. The Case 1 simulation considers the simplest conditions where the entire stratum is modeled as a single layer. The average value of e_o for the stratum was specified for one sample point at midheight and CS3 used this value to calculate the remaining e_o profile, which was nearly linear with depth and deviated only slightly from the stratum average (Fig. 15). The k_o profile was similarly calculated, with the stratum average obtained from the k_o profile provided by Hinchberger and Rowe (1998) and the remaining k_o profile calculated from e_o values and C'_k (Fig. 16). Values of C_c, C_r, and C'_k were each constant and equal to the respective stratum averages (Table 6, Fig. 17). Leroueil et al. (1983) established that the measured preconsolidation stress for Gloucester clays is strain-rate dependent, which is not taken into account by CS3. To partly compensate for this effect, the σ'_p profile of Hinchberger and Rowe (1998), in which measured oedometer values were corrected for strain-rate effects (14% reduction), was used for each simulation. Fig. 18 presents this σ'_p profile along with the σ'_o profile calculated by CS3. A uniform stress increment of 48.4 kPa was applied to the compressible stratum for Case 1 and produced a corresponding uniform distribution of initial excess pore pressure of equal value. This uniform stress increment was calculated using Eq. (10) and stress increment values at the top, middle, and bottom of the stratum as obtained from elastic theory.

Case 2 includes several refinements to the Case 1 analysis. The stratum was modeled using 7 layers, the applied stress increment profile was calculated using elastic theory (i.e., depth-dependent), and average values of e_o, C_c, C_r, and k_o were specified for each layer (Table 5). Sample points for e_o and k_o were specified at the midheight of each layer (Figs. 15 and 16). Case 3 is identical to Case 2 except that the effects of lateral strain on pore pressure generation were taken into account. Lateral strains may be important, considering that the ratio of vertical to horizontal displacements at the base of the fill midway between the shoulder and toe was approximately 4.4 (Bozozuk 1972). Immediate settlements were calculated using elastic theory with a Young's modulus of 19.2 MPa, Poisson's ratio of 0.4, and net applied stress increment of 43.5 kPa (Bozozuk and Leonards 1972). Consolidation settlements were calculated using CS3 and the Skempton-Bjerrum correction (Skempton and Bjerrum 1957) with layer-average pore pressure parameters A (Table 5) provided by Bozozuk (1972) and changes in vertical and horizontal total stresses ($\Delta\sigma_1$ and $\Delta\sigma_3$) given by elastic theory. A small change to the CS3 code was needed to accommodate the Skempton-Bjerrum correction. Finally, Case 4 represents the most sophisticated analysis and is identical to Case 3 except that C'_k was defined using layer-average values (Table 5).

Measured heave for the excavation (gauge S1) after unloading was 4 mm and calculated values obtained using CS3 are 13, 24, 19, and 18 mm for Cases 1–4, respectively, which suggests that the C_r values based on laboratory tests (Bozozuk 1972) may be overestimated. The immediate settlement measured for gauge S1 (26 mm) is in good agreement with the calculated value based on elastic theory (24 mm) for Cases 3 and 4. Field settlement measurements and corresponding settlement curves obtained using CS3 are shown for gauges S1–S3 in Fig. 19. Interestingly, the CS3 curves for all four cases provide a reasonable first approximations to the measured data. This suggests that specific details for the various simulated cases are not critically important for this field study, which likely occurs because all simulations used the same Hinchberger and Rowe (1998) profile for preconsolidation stress. All simulated curves for the deepest gauge (S3) underestimate the measured settlements, especially after 3,000 days. For gauges S1 and S2, measured settlements are underestimated by Cases 1 and 3 and overestimated by Case 2. The Case 4 simulations, which were the most detailed, provide the closest estimates of measured settlements at S1 and S2. The CS3 curves also indicate that, for this case study, consideration of lateral strain effects reduces the calculated value of total settlement after about 400 days. Although the good agreement for the Case 4 simulation may be fortuitous, analysis of the Gloucester test fill demonstrates the capability of CS3 to provide estimates of consolidation settlement for complex conditions involving layered soils.

Table 6. Analysis Methods for Gloucester Test Fill

Parameter	Case 1	Case 2	Case 3	Case 4
R_i	1	7	7	7
Applied stress	Uniform (48.4 kPa)	Depth-dependent (elastic theory)	Depth-dependent (elastic theory)	Depth-dependent (elastic theory)
Immediate settlement	Not included	Not included	Included	Included
Skempton-Bjerrum (1957) correction	Not included	Not included	Included	Included
e_o	Depth-dependent, stratum average at midheight (2.07)	Depth-dependent, layer averages at midheights (Table 5)	Depth-dependent, layer averages at midheights (Table 5)	Depth-dependent, layer averages at midheights (Table 5)
σ'_p	Hinchberger and Rowe (1998)	Hinchberger and Rowe (1998)	Hinchberger and Rowe (1998)	Hinchberger and Rowe (1998)
C_c	Stratum average (2.09)	Layer average (Table 5)	Layer average (Table 5)	Layer average (Table 5)
C_r	Stratum average (0.073)	Layer average (Table 5)	Layer average (Table 5)	Layer average (Table 5)
k_o	Depth-dependent, stratum average at midheight (1.17×10^{-9} m/s)	Depth-dependent, layer averages at midheights (Table 5)	Depth-dependent, layer averages at midheights (Table 5)	Depth-dependent, layer averages at midheights (Table 5)
C'_k	Stratum average (2.7)	Stratum average (2.7)	Stratum average (2.7)	Layer average (Table 5)

Conclusions

The following conclusions are reached as a result of the development of CS3 and subsequent investigations of consolidation behavior using this model:

1. CS3 is a numerical model for one-dimensional large strain consolidation of layered soils. The algorithm accounts for vertical strain, soil self-weight, changing material properties during consolidation, unload/reload, time-dependent loading and boundary conditions, an externally applied hydraulic gradient, and variable profiles for preconsolidation stress and applied stress increment. CS3 utilizes constitutive relationships defined in terms of conventional parameters, as opposed to individual data points in CS2, and allows for direct input of laboratory and field data to facilitate modeling for practical applications.
2. Verification checks of CS3 show excellent agreement with available analytical and numerical solutions.
3. Layered soil heterogeneity can have important effects on calculated settlement and distribution of excess pore pressure. Characterization of a multilayer system as a single layer with average properties may result in significant errors.
4. Settlement estimates obtained using CS3 are in good agreement with field measurements for the Gloucester test fill and demonstrate the general capability of CS3 for analysis of complex conditions involving layered soils.

Acknowledgments

Financial support for this investigation was provided by Grant No. CMMI-1001023 from the Geotechnical Engineering Program of the U.S. National Science Foundation. This support is gratefully acknowledged. The authors also thank Dr. R. Kerry Rowe, Professor of the Department of Civil Engineering at Queen's University, for providing additional information about the Gloucester test fill.

Notation

The following symbols are used in this paper:

A = Skempton pore pressure parameter;
a_v = coefficient of compressibility;
C_c = compression index;
C'_k = reciprocal of hydraulic conductivity change index;
C_r = recompression index;
c_v = coefficient of consolidation;
e = void ratio;
e_o = initial void ratio;
e_{os} = initial void ratio of soil sample;
e_p = preconsolidation void ratio;
F = stress distribution factor for depth-dependent loading;
F_b = stress distribution factor at stratum base;
F_m = stress distribution factor at stratum middle;
F_t = stress distribution factor at stratum top;
G_s = specific gravity of solids;
H_i = height of ith layer;
$H_{i,o}$ = initial height of ith layer;
H_T = height of stratum;
H_{To} = initial height of stratum;
h = total head;
h_b = total head at bottom boundary;
h_{bo} = initial total head at bottom boundary;
h_t = total head at top boundary;
h_{to} = initial total head at top boundary;
i,j = element coordinate;
k = vertical hydraulic conductivity;
k_o = initial vertical hydraulic conductivity;
k_{os} = initial vertical hydraulic conductivity of soil sample;
L = height of element;
L_o = initial height of element;
p_o = initial depth-dependent vertical effective stress at top boundary;
q_o = initial depth-independent vertical effective stress at top boundary;
R_i = number of layers in stratum;
$R_{j,i}$ = number of elements in ith layer;
R_T = number of elements in whole stratum;
S = consolidation settlement of stratum;
S_t = total settlement of stratum;
S_{ult} = ultimate consolidation settlement of stratum;

t = time;
U_{avg} = average degree of consolidation;
u = pore pressure;
u_{ex} = excess pore pressure;
v_{rf} = relative discharge velocity;
z = vertical coordinate;
z_i = layer elevation;
z_o = initial elevation of element node;
γ = saturated unit weight of soil;
γ'_o = initial buoyant unit weight of soil;
γ_w = unit weight of water;
Δp = change in depth-dependent vertical effective stress at top boundary;
Δq = change in depth-independent vertical effective stress at top boundary;
Δq_{avg} = average vertical effective stress change across soil stratum;
Δt = time increment;
$\Delta\sigma'_b$ = change in vertical effective stress at bottom of soil stratum;
$\Delta\sigma'_m$ = change in vertical effective stress in middle of soil stratum;
$\Delta\sigma'_t$ = change in vertical effective stress at top of soil stratum;
σ = vertical total stress;
σ' = vertical effective stress;
σ'_o = initial vertical effective stress;
σ'_p = preconsolidation stress; and
σ'_{ps} = preconsolidation stress of soil sample.

Superscripts

t = time;
$\sim$ = data points for depth-independent loading schedule; and
$-$ = data points for depth-dependent loading schedule.

Subscripts

a = summation index;
b = summation index;
i = ith layer;
i,j = jth element of ith layer; and
s = sample.

References

Al-Tabbaa, A., and Wood, D. M. (1987). "Some measurements of the permeability of kaolin." *Géotechnique*, 37(4), 499–503.

Aydilek, A. H., Edil, T. B., and Fox, P. J. (2000). "Consolidation characteristics of wastewater sludge." *Geotechnics of high water content materials, special technical publication 1374*, T. B. Edil and P. J. Fox, eds., ASTM, West Conshohocken, PA, 309–323.

Azzouz, A. S., Krizek, R. J., and Corotis, R. B. (1976). "Regression analysis of soil compressibility." *Soils Found.*, 16(2), 19–29.

Berilgen, M. M., Ozaydin, I. K., and Edil, T. B. (2000). "A case history: Dredging and disposal of Golden Horn sediments." *Geotechnics of high water content materials, special technical publication 1374*, T. B. Edil and P. J. Fox, eds., ASTM, West Conshohocken, PA, 324–336.

Berilgen, S. A. (2004). "Determination of consolidation behavior of halic dredged material by using a seepage induced consolidation testing system." *J. Eng. and Natural Sciences*, 3(3), 60–72.

Berilgen, S. A., Biçer, P., Berilgen, M. M., and Özaydin, K. I. (2006). "Assessment of consolidation behavior of Golden Horn marine dredged material." *Mar. Georesour. Geotechnol.*, 24(1), 1–16.

Berles, J. D. (1995). "A numerical model for the consolidation of clay." M.S.C. E. thesis, School of Civil Engineering, Purdue Univ., West Lafayette, IN.

Bharat, T. V., and Sharma, J. (2011). "Prediction of compression and permeability characteristics of mine tailings using natural computation and large-strain consolidation framework." *Proc., Geo-Frontiers 2011*, ASCE, Reston, VA, 3868–3877.

Bicer, P. (2005). "Geotechnical characteristics of soils having high water content." *J. Eng. and Natural Sciences*, 2(2), 51–63.

Bozozuk, M. (1972). "The Gloucester test fill." Ph.D. thesis, Purdue Univ., West Lafayette, IN.

Bozozuk, M., and Leonards, G. A. (1972). "The Gloucester test fill." *Proc., ASCE Specialty Conf. on Performance of Earth and Earth-Supported Structures*, ASCE, New York, 299–317.

Chen, R. P., Zhou, W. H., Wang, H. Z., and Chen, Y. M. (2005). "One-dimensional nonlinear consolidation of multi-layered soil by differential quadrature method." *Comput. Geotech.*, 32(5), 358–369.

Fox, P. J. (2000). "CS4: A large strain consolidation model for accreting soil layers." *Geotechnics of high water content materials, special technical publication 1374*, T. B. Edil and P. J. Fox, eds., ASTM, West Conshohocken, PA, 29–47.

Fox, P. J. (2007a). "Coupled large strain consolidation and solute transport. I: Model development." *J. Geotech. Geoenviron. Eng.*, 10.1061/(ASCE)1090-0241(2007)133:1(3), 3–15.

Fox, P. J. (2007b). "Coupled large strain consolidation and solute transport. II: Model verification and simulation results." *J. Geotech. Geoenviron. Eng.*, 10.1061/(ASCE)1090-0241(2007)133:1(16), 16–29.

Fox, P. J., and Berles, J. D. (1997). "CS2: A piecewise-linear model for large strain consolidation." *Int. J. Numer. Anal. Methods Geomech.*, 21(7), 453–475.

Fox, P. J., Di Nicola, M., and Quigley, D. W. (2003). "Piecewise-linear model for large strain radial consolidation." *J. Geotech. Geoenviron. Eng.*, 10.1061/(ASCE)1090-0241(2003)129:10(940), 940–950.

Fox, P. J., and Lee, J. (2008). "Model for consolidation-induced solute transport with nonlinear and nonequilibrium sorption." *Int. J. Geomech.*, 10.1061/(ASCE)1532-3641(2008)8:3(188), 188–198.

Fox, P. J., Lee, J., and Qiu, T. (2005). "Model for large strain consolidation by centrifuge." *Int. J. Geomech.*, 10.1061/(ASCE)1532-3641(2005)5:4(267), 267–275.

Fox, P. J., and Pu, H. (2012). "Enhanced CS2 model for large strain consolidation." *Int. J. Geomech.*, 10.1061/(ASCE)GM.1943-5622.0000171, 574–583.

Fox, P. J., Pu, H.-F., and Christian, J. T. (2014). "Evaluation of data analysis methods for the CRS consolidation test." *J. Geotech. Geonviron. Eng.*, 10.1061/(ASCE)GT.1943-5606.0001103, 04014020.

Fox, P. J., and Qiu, T. (2004). "Model for large strain consolidation with compressible pore fluid." *Int. J. Numer. Anal. Methods Geomech.*, 28(11), 1167–1188.

Gibson, R. E., England, G. L., and Hussey, M. J. L. (1967). "The theory of one-dimensional consolidation of saturated clays. I. Finite non-linear consolidation of thin homogeneous layers." *Géotechnique*, 17(3), 261–273.

Hazzard, J. F., Yacoub, T. E., and Curran, J. (2008). "Consolidation in multi-layered soils: A hybrid computation scheme." *Proc., GeoEdmonton '08: 61st Canadian Geotechnical Conf.,* 182–189.

Hinchberger, S. D., and Rowe, R. K. (1998). "Modelling the rate-sensitive characteristics of the Gloucester foundation soil." *Can. Geotech. J.*, 35(5), 769–789.

Kim, H.-J., and Mission, J. L. (2011). "Numerical analysis of one-dimensional consolidation in layered clay using interface boundary relations in terms of infinitesimal strain." *Int. J. Geomech.*, 10.1061/(ASCE)GM.1943-5622.0000066, 72–77.

Kokusho, T., and Kojima, T. (2002). "Mechanism for postliquefaction water film generation in layered sand." *J. Geotech. Geoenviron. Eng.*, 10.1061/(ASCE)1090-0241(2002)128:2(129), 129–137.

Kulhawy, F. H., and Mayne, P. W. (1990). "Manual on estimating soil properties for foundation design." *Rep. EPRI EL-6800*, Electric Power Research Institute, Palo Alto, CA.

Kwon, Y., Kazama, M., and Uzuoka, R. (2007). "Geotechnical hybrid simulation system for one-dimensional consolidation analysis." *Soils Found.*, 47(6), 1133–1140.
Lee, J., and Fox, P. J. (2005). "Efficiency of seepage consolidation for preparation of clay substrate for centrifuge testing." *J. ASTM Geotech Test.*, 28(6), 577–585.
Lee, J., and Fox, P. J. (2009). "Investigation of consolidation-induced solute transport. II: Experimental and numerical results." *J. Geotech. Geoenviron. Eng.*, 10.1061/(ASCE)GT.1943-5606.0000048, 1239–1253.
Lee, J., and Park, J.-W. (2013). "Numerical investigation for the isolation effect of in situ capping for heavy metals in contaminated sediments." *KSCE J. Civ. Eng.*, 17(6), 1275–1283.
Lee, K., and Sills, G. C. (1979). "A moving boundary approach to large strain consolidation of a thin soil layer." *Proc., 3rd Int. Conf. on Numerical Methods in Geomechanics*, Balkema, Rotterdam, Netherlands, 163–173.
Lee, P. K. K., Xie, K. H., and Cheung, Y. K. (1992). "A study on one-dimensional consolidation of layered systems." *Int. J. Numer. Anal. Methods Geomech.*, 16(11), 815–831.
Leroueil, S., Samson, L., and Bozozuk, M. (1983). "Laboratory and field determination of preconsolidation pressures at Gloucester." *Can. Geotech. J.*, 20(3), 477–490.
Lewis, T. W. (2009). "Theoretical effects of consolidation on solute transport in soil barriers." Ph.D. thesis, Univ. of Newcastle, Callaghan, NSW, Australia.
Lo, K. Y., Bozozuk, M., and Law, K. T. (1976). "Settlement analysis of the Gloucester test fill." *Can. Geotech. J.*, 13(4), 339–354.
Meric, D., Hellweger, F., Barbuto, S., Rahbar, N., Alshawabkeh, A. N., and Sheahan, T. C. (2013). "Model prediction of long-term reactive core mat efficacy for capping contaminated aquatic sediments." *J. Environ. Eng.*, 10.1061/(ASCE)EE.1943-7870.0000635, 564–575.
Meric, D., Sheahan, T. C., Alshawabkeh, A., and Shine, J. (2010). "A consolidation and contaminant transport device for assessing reactive mat effectiveness for subaqueous sediment remediation." *J. ASTM Geotech Test.*, 33(6), 423–433.
Mesri, G., and Choi, Y. K. (1985). "Settlement analysis of embankments on soft clays." *J. Geotech. Engrg.*, 10.1061/(ASCE)0733-9410(1985)111:4(441), 441–464.
Mesri, G., Lo, D. O. K., and Feng, T.-W. (1994). "Settlement of embankments on soft clays." *Vertical and horizontal deformations of foundations and embankments, Geotechnical Special Publication No. 40*, A. T. Yeung and G. Y. Félio, eds., ASCE, Reston, VA, 8–56.
Nagaraj, T. S., Pandian, N. S., and Narasimha Raju, P. S. R. (1994). "Stress-state—permeability relations for overconsolidated clays." *Géotechnique*, 44(2), 349–352.
Nogami, T., and Li, M. (2002). "Consolidation of system of clay and thin sand layers." *Soils Found.*, 42(4), 1–11.
Nogami, T., and Li, M. (2003). "Consolidation of clay with a system of vertical and horizontal drains." *J. Geotech. Geoenviron. Eng.*, 10.1061/(ASCE)1090-0241(2003)129:9(838), 838–848.
Perrone, V. J. (1998). "One dimensional computer analysis of simultaneous consolidation and creep of clay." Ph.D. thesis, Virginia Polytechnic Institute and State Univ., Blacksburg, VA.
Pu, H.-F., Fox, P. J., and Liu, Y. (2013). "Model for large strain consolidation under constant rate of strain." *Int. J. Numer. Anal. Methods Geomech.*, 37(11), 1574–1590.
Qiu, T., and Fox, P. J. (2008). "Numerical analysis of 1-D compression wave propagation in saturated poroelastic media." *Int. J. Numer. Anal. Methods Geomech.*, 32(2), 161–187.
Schiffman, R. L., and Stein, J. R. (1970). "One-dimensional consolidation of layered systems." *J. Soil Mech. and Found. Div.*, 96(4), 1499–1504.
Skempton, A. W., and Bjerrum, L. (1957). "A contribution to the settlement analysis of foundations on clay." *Géotechnique*, 7(4), 168–178.
Tang, X. W., and Onitsuka, K. (2001). "Consolidation of double-layered ground with vertical drains." *Int. J. Numer. Anal. Methods Geomech.*, 25(14), 1449–1465.
Tavenas, F., Jean, P., Leblond, P., and Leroueil, S. (1983). "The permeability of natural soft clays. Part II: Permeability characteristics." *Can. Geotech. J.*, 20(4), 645–660.
Townsend, F. C., and McVay, M. C. (1990). "SOA: Large strain consolidation predictions." *J. Geotech. Engrg.*, 10.1061/(ASCE)0733-9410(1990)116:2(222), 222–243.
Walker, R., Indraratna, B., and Sivakugan, N. (2009). "Vertical and radial consolidation analysis of multilayered soil using the spectral method." *J. Geotech. Geoenviron. Eng.*, 10.1061/(ASCE)GT.1943-5606.0000075, 657–663.
Wang, X. S., and Jiao, J. J. (2004). "Analysis of soil consolidation by vertical drains with double porosity model." *Int. J. Numer. Anal. Methods Geomech.*, 28(14), 1385–1400.
Xie, K. H., Xie, X. Y., and Gao, X. (1999). "Theory of one dimensional consolidation of two-layered soil with partially drained boundaries." *Comput. Geotech.*, 24(4), 265–278.
Xie, K. H., Xie, X. Y., and Jiang, W. (2002). "A study on one-dimensional nonlinear consolidation of double-layered soil." *Comput. Geotech.*, 29(2), 151–168.
Zhou, Y., Deng, A., and Wang, C. (2013). "Finite-difference model for one-dimensional electro-osmotic consolidation." *Comput. Geotech.*, 54, 152–165.
Zhu, G., and Yin, J.-H. (1999a). "Consolidation of double soil layers under depth-dependent ramp load." *Géotechnique*, 49(3), 415–421.
Zhu, G., and Yin, J.-H. (1999b). "Finite element analysis of consolidation of layered clay soils using an elastic visco-plastic model." *Int. J. Numer. Anal. Methods Geomech.*, 23(4), 355–374.